A&A 543, A137 (2012)
DOI: 10.1051/0004-6361/201218810

Astronomy & Astrophysics

The birth rate of supernovae from double-degenerate and core-degenerate systems

X. Meng[1,2] and W. Yang[1,3]

[1] School of Physics and Chemistry, Henan Polytechnic University, 454000 Jiaozuo, PR China
e-mail: xiangcunmeng@hotmail.com
[2] Key Laboratory for the Structure and Evolution of Celestial Objects, Chinese Academy of Sciences, 650011 Kunming, PR China
[3] Department of Astronomy, Beijing Normal University, 100875 Beijing, PR China

Received 12 January 2012 / Accepted 10 May 2012

ABSTRACT

Context. Some recent observations of the delay-time distribution (DTD) of Type Ia supernovae (SNe Ia) seem to uphold the double-degenerate (DD) scenario as the progenitor model of SNe Ia, but the core-degenerate (CD) scenario remains a strong competitor to the DD one.

Aims. We investigate the effects of metallicity and the different treatments of common envelope (CE) on the DTD of SNe Ia by considering the DD and CD scenarios, and check the suggestion that the total mass of DD system is the main dependent variable of Phillips relation.

Methods. We perform a series of Monte Carlo simulations based on a rapid binary evolution code and consider two treatments of CE evolution, i.e. α-formalism and γ-algorithm.

Results. We find that only when the α-formalism is considered with a high CE ejection efficiency, may the shape of the DTD for DD systems be consistent with that derived observationally, i.e. a power law of $\sim t^{-1}$, while the value of the birth rate of SNe Ia marginally matches observations. For the α-formalism with a low CE ejection efficiency and the γ-algorithm, neither the shape of the DTD nor the value of the birth rate can be compared with those of the observations. Metallicity may not have a significant influence on the shape of DTD, but a lower metallicity may lead to a slightly higher birth rate of SNe Ia by a factor of 2, especially for SNe Ia with long delay times. If the results for the single-degenerate (SD) channel are incorporated into those for the DTD, both the shape of DTD and its value may be closely consistent with observations for SNe Ia younger than 2.5 Gyr, and SD and DD channels provide comparable contributions to the total SNe Ia, while for SNe Ia with delay times longer than 2.5 Gyr, DD is the dominant channel and the birth rate is lower than that derived from observations by a factor up to about four. In addition, we calculate the evolutions of various integral parameters of DD systems, and do not find any one suitable to explain the correlation between the brightness of SNe Ia and its delay time. Moreover, there are three channels producing CD systems that may contribute a few SNe Ia, but the contribution of CD systems to the total SNe Ia is no more than 1%.

Conclusions. There may be other channels or mechanisms contributing to SNe Ia with long delay times.

Key words. white dwarfs – supernovae: general – binaries: general – stars: evolution

1. Introduction

Type Ia supernovae (SNe Ia) have been found to be important to many astrophysical fields, especially as principal distance indicators to measure cosmological parameters, where their use resulted in the discovery of the accelerating expansion of the Universe (Riess et al. 1998; Schmidt et al. 1998; Perlmutter et al. 1999). This result was extremely exciting and implied that dark energy exists. At present, SNe Ia are regarded as critical cosmological probes for testing both the evolution of the dark energy equation of state with time and the evolutionary history of the universe (Riess et al. 2007; Kuznetsova et al. 2008; Howell et al. 2009a).

However, the precise nature of SNe Ia remains unclear, especially their progenitor (Hillebrandt & Niemeyer 2000; Leibundgut 2000; Parthasarathy et al. 2007; Wang & Han 2012). There is a consensus that SNe Ia result from the thermonuclear explosion of a carbon-oxygen (CO) white dwarf (WD) in a binary system (Hoyle & Fowler 1960). According to the nature of the companions of the mass-accreting WDs, two possible progenitors of SNe Ia have been discussed over the past three decades, i.e. the single-degenerate (SD) model where the companion is a normal star (Whelan & Iben 1973; Nomoto et al. 1984), and the double-degenerate (DD) model where a CO WD merges with another CO WD (Iben & Tutukov 1984; Webbink 1984). At present, both models cannot be ruled out completely by observations (see the review by Howell 2011).

To distinguish between these different progenitor models, it is important to measuring the delay-time distribution (DTD), where the delay time is the elapsed time between the primordial system formation and the explosion as a supernova (SN) event and the DTD is the SN birth rate versus their delay time for a single starburst. An increasing amount of observational studies of the DTD of SNe Ia have found that the DTD follows a power-law form of t^{-1} (Totani et al. 2008; Maoz & Mannucci 2011), which is difficult to interpret in terms of the SD model (Meng & Yang 2010a), but in contrast can be naturally explained by the DD model (Yungelson & Livio 2000; Mennekens et al. 2010). Some theoretical and observational studies have shown that metallicity may have a strong influence on the birth rate of

SNe Ia (Khan et al. 2011b; Meng et al. 2011a). We wish to establish the effect of metallicity on the birth rate of SNe Ia in the DD scenario.

When SNe Ia are used as distance indicators, the Phillips relation is adopted, which is a linear relation between the absolute magnitude of SNe Ia at maximum light and the magnitude drop in the B band light curve during the first 15 days following the maximum light (Phillips 1993). This relation was motivated by the observations of two peculiar SN events (SN 1991bg and SN 1991T) and implies that the brightness of SNe Ia is determined mainly by one parameter. The amount of ^{56}Ni formed during the SN explosion dominates the maximum luminosity of SNe Ia (Arnett 1982). However, the origin of the variation in the amount of ^{56}Ni for different SNe Ia is still unclear (Podsiadlowski et al. 2008). Observationally, the most luminous SNe Ia always occur in spiral galaxies, while both spiral and elliptical galaxies host systematically dimmer SNe Ia, which leads to a dimmer mean peak SN brightness in elliptical than spiral galaxies (Hamuy et al. 1996; Brandt et al. 2010). In addition, the mean peak brightness of SNe Ia in a galaxy varies less in the outer than the inner regions (Wang et al. 1997; Riess et al. 1999). In other words, age could be the most important factor in determining the luminosity of SNe Ia, and dimmer SNe Ia have a wide age distribution (Gallagher et al. 2008; Neill 2009; Howell et al. 2009b). From these observations, we concluded that the range and average value of the brightness of SNe Ia decrease with their delay time. If the maximum luminosity of SNe Ia is mainly determined by one parameter as shown by the Phillips relation, we may expect that the range of the parameter decreases, and its average value either increases or decreases with the age of SNe Ia.

Many efforts have been made to resolve this problem. Some multi-dimensional numerical simulations have shown that varying the ignition intensity at the center of WDs or the transition density from deflagration to detonation might enable us to determine the underlying cause of the observed correlation between peak luminosity and light-curve width (Hillebrandt & Niemeyer 2000; Höflich et al. 2006, 2010; Kasen et al. 2010). In addition, the ratio of nuclear-statistical-equilibrium to intermediate-mass elements in the explosion ejecta may be a key parameter in determining the width of SN Ia light curve and its peak luminosity (Pinto & Eastman 2001; Mazzali et al. 2001, 2007). Lesaffre et al. (2006) suggested that the central density of the WD at ignition may be the origin of the Phillips relation in a systematic study of the sensitivity of ignition conditions for H-rich Chandrasekhar-mass single-degenerate exploders to various properties of the progenitors (see also Podsiadlowski et al. 2008), which was upheld by detailed multi-dimensional numerical simulations of explosion (Krueger et al. 2010). Moreover, metallicity may also affect the production of ^{56}Ni, thus the maximum luminosity, both in theory (Timmes et al. 2003; Travaglio et al. 2005; Podsiadlowski et al. 2006; Bravo et al. 2010a) and observations (Branch & Bergh 1993; Hamuy et al. 1996; Wang et al. 1997; Cappellaro et al. 1997; Shanks et al. 2002). On the basis of the suggestion that the ratio of the carbon to oxygen (C/O) of a white dwarf at the moment of explosion could be the dominant parameter determining the production of ^{56}Ni (Nomoto et al. 1999, 2003), Meng & Yang (2011) found that the effects of metallicity and C/O on the production of ^{56}Ni may complement each other. Most of these discussions above focused on the Chandrasekhar mass model, in which the WDs explode as SNe Ia when their masses are close to the Chandrasekhar mass limit. However, the sub-Chandrasekhar mass model may still be able to explain SNe Ia such as 1991bg, as well as normal SNe Ia (Sim et al. 2010; Ruiter et al. 2011). In addition, observations of several very bright SNe Ia implied that their progenitor WDs might have a super-Chandrasekhar mass (Astier et al. 2006; Howell et al. 2006; Hicken et al. 2007; Scalzo et al. 2010; Yuan et al. 2010; Tanaka et al. 2010; Yamanaka et al. 2010). Although these very bright SNe Ia may also be explained in terms of the SD scenario (Chen & Li 2009; Liu et al. 2009; Hachisu et al. 2012), that the DD systems are the progenitor of the very bright SNe Ia still cannot be completely ruled out at present. Howell (2011) suggested that the DD scenario has a natural explanation of the higher SN luminosity in young environments, i.e. younger, more massive stars produce more massive white dwarfs that have more potential fuel than less massive mergers, and then produce a bright SNe Ia (see also Maoz & Mannucci 2011). This suggestion still needs to be checked carefully.

However, earlier numerical simulations showed that the most probable fate of the DD merger is an accretion-induced collapse (AIC) and, finally, neutron star formation (see the review by Hillebrandt & Niemeyer 2000). Even if the merger survived the AIC, a super wind from giant-like structure before supernova explosion would occur and the remnant might lose about 0.5 $M_{\odot}$ and shrink in mass to below the critical mass for explosion (Soker 2011). Following the suggestion of Sparks & Stecher (1974) and Livio & Riess (2003), Kashi & Soker (2011) developed a core-degenerate (CD) model to overcome the drawbacks of the DD model, in which a white dwarf merges with the core of an asymptotic giant branch (AGB) star shortly after a common envelope (CE) phase. However, they did not consider the evolution of the birth rate from the CD supernova. In this paper, we study the evolution in terms of a detailed binary population synthesis (BPS) study.

In Sect. 2, we simply describe our method, and present the calculation results in Sects. 3 and 4. In Sect. 5, we show our discussions and main conclusions.

2. METHOD

2.1. Common envelope

The CE phase is very important to the formation of DD systems. During binary evolution, the mass ratio ($q = M_{\rm donor}/M_{\rm accretor}$) is a crucial parameter. If it is larger than a critical mass ratio, $q_{\rm c}$, mass transfer between the two components is dynamically unstable and a CE forms (Paczyński 1976). The ratio $q_{\rm c}$ varies with the evolutionary state of the donor star at the onset of Roche lobe overflow (RLOF) (Hjellming & Webbink1987; Webbink 1988; Han et al. 2002; Podsiadlowski et al. 2002; Chen & Han 2008). In this study, we adopted $q_{\rm c} = 4.0$ when the donor star is on the main sequence (MS) or crossing the Hertzsprung gap (HG). This value is supported by detailed binary evolution studies (Han et al. 2000; Chen & Han 2002, 2003). If the donor star is on either the first giant branch (FGB) or the AGB, we use

$$q_{\rm c} = \left[1.67 - x + 2\left(\frac{M_{\rm c}}{M}\right)^5\right]/2.13, \quad (1)$$

where $M_{\rm c}$ is the core mass of the donor star, and $x = {\rm d}\ln R_1/{\rm d}\ln M$ is the mass–radius exponent of the donor star, which varies with composition. If the mass donors are naked helium giants, then $q_{\rm c} = 0.748$ based on Eq. (1) (see Hurley et al. 2002 for details).

Embedded in the CE are the dense core of the donor star and the secondary. Owing to frictional drag with the envelope, the orbit of the embedded binary decays, and a large part of the orbital energy released in the spiral-in process is injected into the envelope (Livio & Soker 1988).

The CE evolution is very complicated and different authors may use different methods to treat it in their BPS studies. There are two dominant methods for treating the CE evolution, i.e. the α-formalism ensuring energy balance and the γ-algorithm ensuring angular momentum balance. The α-formalism, which is widely used, may closely reproduce the orbital-period distribution of WD + MS systems as noted by Zorotovic et al. (2010) (see also Hurley et al. 2002 and Webbink 2008), while it may be unable to describe the production of a close pair of white dwarfs. To solve this problem, Nelemans et al. (2000) and Nelemans & Tout (2005) developed the γ-algorithm, which may explain the formation of all kinds of close binaries. In this paper, both of these descriptions are applied.

For the α-formalism, the final orbital separation $a_{\rm f}$ after CE phase is obtained by

$$\frac{a_{\rm f}}{a_{\rm i}}=\frac{M_{\rm c}}{M}\left(1+\frac{2M_{\rm e}a_{\rm i}}{\alpha_{\rm CE}\lambda mR_{1}}\right)^{-1}, \quad (2)$$

where $a_{\rm i}$ is the initial orbital separation at the onset of the CE, the masses M, $M_{\rm c}$, and $M_{\rm e}$ are those of the donor, the donor core, and the envelope, respectively, R_1 is the radius of the donor, and m is the companion mass. The parameter $\alpha_{\rm CE}$ is the CE ejection efficiency, i.e. the fraction of the released orbital energy used to eject the CE, and λ is a structure parameter relying on the evolutionary stage of the donor. At present, the value of $\alpha_{\rm CE}$ is very uncertain and may vary from 0.4 to 3.0 (see the review of Ivanova 2011). Because the thermal energy in the envelope is not incorporated into the binding energy in this paper, $\alpha_{\rm CE}$ may be greater than 1 (see Han et al. 1995 for details about the thermal energy). In this paper, we set $\alpha_{\rm CE}$ to either 1.0 or 3.0 when studying the DD and CD scenarios, and $\alpha_{\rm CE}$ = 1.5 or 2.0 were also tested. For λ, we assumed that it is a constant (λ = 0.5, de Kool et al. 1987).

In the γ-algorithm, $a_{\rm f}$ was obtained from

$$\frac{a_{\rm f}}{a_{\rm i}}=\left(\frac{M}{M_{\rm c}}\right)^{2}\left(\frac{M_{\rm c}+m}{M+m}\right)\left(1-\gamma_{\rm CE}\frac{M_{\rm e}}{M+m}\right)^{2}. \quad (3)$$

where $\gamma_{\rm CE}$ is a free parameter. Based on the results of Nelemans & Tout (2005), we set $\gamma_{\rm CE}$ = 1.5.

2.2. Basic parameters of our Monte Carlo simulations

To investigate the birthrate of SNe Ia in DD systems, we followed the evolution of 1×10^{7} binaries via Hurley's rapid binary evolution code (Hurley et al. 2000, 2002). The primordial binary samples are generated in a Monte Carlo way and a circular orbit was assumed for all binaries. The basic parameters for the simulations were as follows: (1) a constant star formation rate (SFR) of 5 $M_{\odot}\,{\rm yr}^{-1}$ over the past 15 Gyr or a single starburst of 10^{11} $M_{\odot}$; (2) the initial mass function (IMF) of Miller & Scalo (1979); (3) a constant mass-ratio distribution; (4) all stars are members of binary systems and the distribution of separations is constant in $\log a$ for wide binaries, where a is the orbital separation, and falls off smoothly at small separations, where a = 10 $R_{\odot}$ is the boundary for wide and close binaries; (5) metallicities were chosen to be Z = 0.02, 0.002, and 0.0001 (see Meng & Yang 2010a for details of these input parameters).

We tracked the evolutions of the 1×10^{7} binaries until they become DD systems. Following the DD system, gravitational wave radiation (GWR) dominates the evolution of the system on a timescale $t_{\rm GW}$ (Landau & Lifshitz 1962)

$$t_{\rm GW}({\rm yr})=8\times10^{7}\times\frac{(M_1+M_2)^{1/3}}{M_1M_2}P^{8/3}, \quad (4)$$

where P is the orbital period of the DD system in hours, and M_1 and M_2 are the masses of the two WDs in solar masses, respectively. The time elapsed from the birth of primordial binary system to the occurrence of SN Ia was then assumed to be equal to the sum of the timescale on which the primordial secondary star becomes a WD and the orbital decay time. We assume that if the total mass of a DD system is $M_{\rm t}=M_1+M_2\geq1.378\,M_{\odot}$ and the elapsed time is shoter than 15 Gyr, a SN Ia is produced.

2.3. Evolution channel for the CD system

A system consisting of a WD and an AGB core survives a CE phase and then merges shortly after. The core is more massive than the WD and when the merging process starts, it is still very hot and has a larger radius than the cold WD. Hence, the core may be destroyed to form an accretion disk around the WD. Since the less massive WD has a shallower gravitational potential, the temperature in the accretion disk does not reach the ignition temperature and AIC can be avoided. This scenario is only applicable when the merging process occurs within about 10^5 yr of the CE phase. The merger is unlikely to explode soon until a large part of the angular momentum is lost by means of the magneto-dipole radiation torque (see Ilkov & Soker 2012 for details). Thus, as mentioned in Soker (2011), three key factors distinguishing the CD scenario from the DD channel are that in the former scenario: (1) the hot core is more massive than its cold companion WD, (2) the CD system will merge within $\sim10^5$ yr after the CD system forms[1], and (3) its delay time is mainly due to the spinning-down time of the merger product, which results from a magneto-dipole radiation torque (Ilkov & Soker 2012). Ilkov & Soker (2012) and Soker (2011) only introduced one channel to produce CD systems. Three channels could actually produce CD systems, fulfilling the above criteria. However, different treatments of CE may trigger different channels as follows. In the following description, the *primary* is the more massive star in a primordial binary system, while the *secondary* is the less massive one.

Case 1: (wind + RL + CE) This channel can be encountered by both α-formalism and γ-algorithm, but is more common for γ-algorithm, and is similar to that described in Soker (2011) and Ilkov & Soker (2012), which includes two sub-channels. For sub-channel A, the primordial zero-age main sequence (ZAMS) mass of a primary is in the range from 4.0 $M_{\odot}$ to 5.0 $M_{\odot}$, and the mass ratio (m_2/m_1) is relatively high(0.85–0.95). The primordial binary system has a very wide separation (wider than 2300 $R_{\odot}$), which permits the primary to evolve into the thermal pulsing asymptotic giant branch (TPAGB). Before the primary fills its Roche lobe, it loses a lot of material by its wind, which results in the following stable RLOF[2]. At this stage, the secondary is still a MS star. The system becomes a CO WD + MS system after the RLOF. The MS secondary then has a mass higher than the primordial mass of the primary. The WD + MS system continues to evolve and the MS secondary fills its Roche lobe when

[1] Note that the time here is the GWR timescale after the CD system forms and is not the delay time of a SN Ia.

[2] The treatment of RLOF in the Hurley's rapid binary evolution code is a substantially revised version of that presented by Tout et al. (1997) and the radius-mass exponent ζ defined by Webbink (1985) is used to describe the stability of mass transfer.

it becomes a AGB star. Because of the large mass ratio at this stage, the system enters a CE phase. If the CE can be ejected, a CD system forms and merges within $\sim 10^6$ yr.

For sub-channel B, the primordial primary usually has a mass of 3.0–3.5 $M_\odot$, and the mass ratio is higher than 0.99. However, the primordial separation for sub-channel B is not as wide as that for the sub-channel A (1800 $R_\odot$–2100 $R_\odot$). The evolutionary path of the sub-channel B is much similar to that of the sub-channel A and the difference is that when the primary becomes an AGB star, the secondary is a horizontal branch (HB) star (central helium burning), not a MS star.

Case 2: (RL + 4CE) This channel is only encountered when γ-algorithm is adopted. The primordial primary has a mass higher than 6.5 $M_\odot$ and the mass ratio is larger than 0.94, even close to 1, but the primordial separation is only about 100 $R_\odot$. Owing to the small separation, when the primary crosses the HG, it fills its Roche lobe and a stable RLOF occurs, which results in the secondary being more massive than the primordial primary. The separation of the components then increases during the stable mass transfer, the primary continues to evolve to the FGB, and the mass transfer then becomes unstable, leading to the first CE. After the CE ejection, the system consists of a naked helium star and a MS star. According to the γ-algorithm, the separation does not shrink greatly after the first CE ejection. Shortly afterwards, the MS star evolves to the FGB and fills its Roche lobe where the mass transfer is dynamically unstable, and the system then enters into the second CE phase. After the CE ejection, the secondary also becomes a naked helium star, and the system consists of two helium stars. The mass of the helium star from the secondary is higher than that of the primary because the secondary at the MS stage is more massive than the primordial primary for prior stable RLOF ($m_1 \in [1.22, 1.35]$ $M_\odot$ and $m_2 \in [1.4, 1.6]$ $M_\odot$, respectively). The helium star from the primary firstly exhausts its central helium and then begins to cross the helium HG. If it fills its Roche lobe, the third CE is expected for a large mass ratio. However, the mass of the third CE is low compared to the two prior CEs, and the third CE evolution cannot shrink the separation significantly. The CE is again ejected and then the primary becomes a CO WD. Helium is also finally exhausted at the center of the second helium star. As the second helium star crosses the helium HG, it also fills its Roche lobe, leading to the fourth CE. After the ejection of the last CE, a CD system forms. Because of the four CE evolutions, the separation of the CD system is so close that the system merges within $\sim 10^6$ yr.

Case 3: (RL + CE + RL/wind + CE) This channel is encountered when an α-formalism is adopted. The primordial primary has a mass of 4.3–5.2 $M_\odot$ and its mass ratio is lower than in the above two cases (0.68–0.78). The range of primordial separations is from 20 $R_\odot$ to 55 $R_\odot$. Because of the small separation, the primary fills its Roche lobe as it crosses the HG, where a stable mass transfer occurs. The primary loses its envelope and becomes a naked helium star. At the same time, the secondary accretes a lot of material, becoming more massive than primordial primary. Owing to the stable RLOF, the separation greatly increases, and the secondary may then evolve to its HG/RGB phase and fill its Roche lobe. The subsequent mass transfer is dynamically unstable and a CE forms. After the CE ejection, the system consists of two naked helium stars, and owing to the prior stable RLOF, the helium star evolving from the secondary is more massive ($m_1 \in [0.7, 0.85]$ $M_\odot$ and $m_2 \in [1.25, 1.6]$ $M_\odot$, respectively). The helium star that evolves from the primary firstly exhausts its central helium and begins to cross the helium HG. At this stage, if the helium star fills its

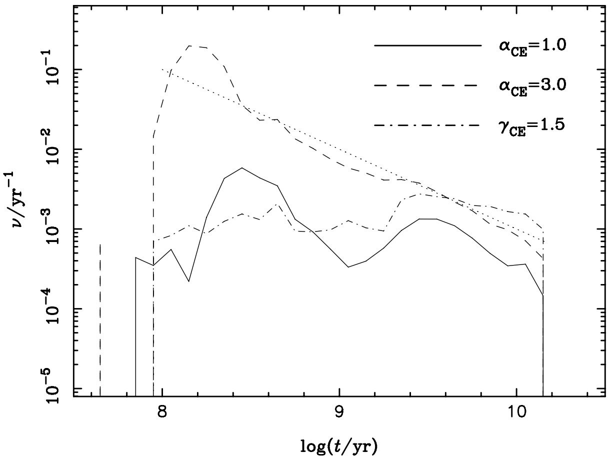

Fig. 1. Evolution of the birthrates of SNe Ia for a single starburst of 10^{11} $M_\odot$, where $Z = 0.02$. Solid, dashed, and dot-dashed lines show the cases with $\alpha_{CE} = 1.0$, $\alpha_{CE} = 3.0$, and $\gamma_{CE} = 1.5$, respectively. The dotted line represents a power-law function of form $f(t) \propto t^{-1}$.

Roche lobe, a stable RLOF occurs and the helium star transfers its envelope onto the second helium star and then becomes a CO WD. It otherwise loses its envelope in terms of a wind to become a WD. The second helium star also finally exhausts its central helium, leading to the expansion of its envelope. Its Roche lobe is then filled and the system enters into the second CE phase for unstable mass transfer. After the CE ejection, a CD system forms and merges within 10^6 yr.

In this paper, we assumed that (1) if a WD produced from a primordial secondary is more massive than its companion WD, the system is a potential CD system; (2) if the potential CD system merges after the emission of GWR within a few $\times\, 10^5$ yr, the merger will explode as a SNe Ia. In addition, to study the birth rate of SNe Ia from CD systems, we traced the evolution of 1×10^8 binaries. To check the influence of the merger timescale by GWR on the birth rate of SNe Ia in the CD system, we considered the cutting time as a free parameter (see Sect. 4).

There is actually a "pollution" channel, that also fulfills our criterion (1) for the potential CD systems. In the channel, the more massive WD also evolves from secondary, but forms earlier than the second WD. The primordial primary has a mass of around 5 $M_\odot$, and the mass ratio is close to 1. The primordial separation is in the range of 130–160 $R_\odot$, which permits the primary to evolve to the FGB. A dynamically unstable mass transfer then results in a CE phase. Following the CE ejection, the system consists of a naked helium star and a MS one. On the basis of the γ-algorithm for CE evolution, the orbital separation does not shrink greatly after the first CE evolution, which permits the secondary to evolve to the early AGB phase, and then the second CE. After the CE is ejected, the secondary becomes a WD and the separation shrinks greatly. After the helium star exhausts its central helium, the helium star also fills its Roche lobe, and the system enters into the third CE phase. After the CE ejection, the system consists of a less massive hot core and a more massive cold WD. The following GWR timescale for the channel may be as long as 1.5 Gyr.

3. Results for a normal DD channel

3.1. Birth rate for a single starburst

In Fig. 1, we show the evolution of the birthrates of SNe Ia from DD systems for a single starburst with $Z = 0.02$, where the

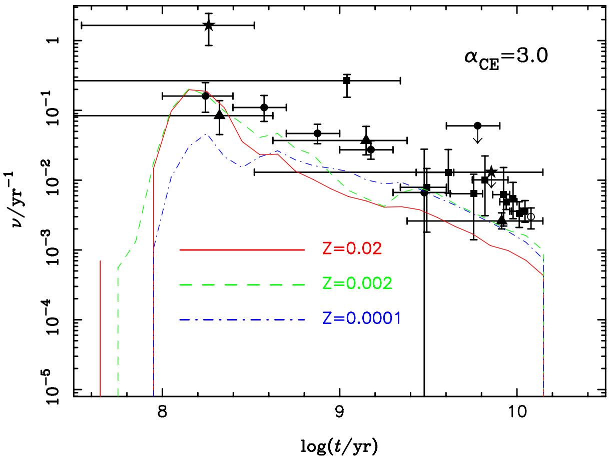

Fig. 2. Evolution of the birthrates of SNe Ia for a single starburst of 10^{11} $M_{\odot}$ with different metallicities, where α_{CE} = 3.0. The circle is from Mannucci et al. (2005), the filled circles are from Totani et al. (2008), stars are from Maoz & Badenes (2010), squares are from Maoz et al. (2010), and triangles are from Maoz et al. (2011).

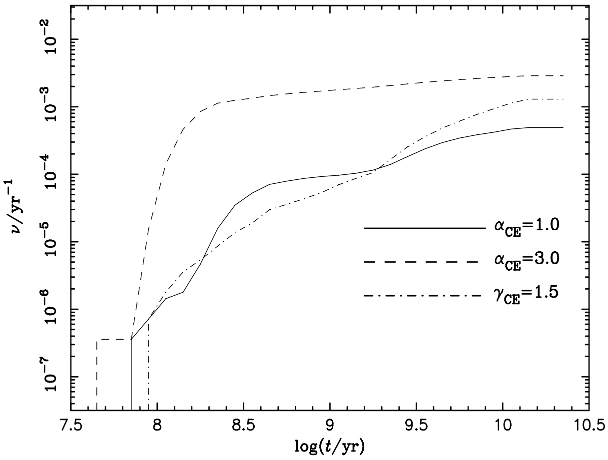

Fig. 3. The evolution of the birth rates of SNe Ia for a constant star formation rate (Z = 0.02, SFR = 5 $M_{\odot}$ yr^{-1}). Solid, dashed, and dot-dashed lines show the cases of α_{CE} = 1.0, α_{CE} = 3.0, and γ_{CE} = 1.5, respectively.

evolution is characterized by a DTD. For comparison, we also show a power-law function of the form $f(t) \propto t^{-1}$ by a dotted line in Fig. 1. We can see from Fig. 1 that the shape of the DTD depends on the treatment of CE. Some recent measurements measure a similar power-law shape with an index of −1 (Maoz & Mannucci 2011). In Fig. 1, only when α_{CE} = 3.0 ($\alpha_{CE}\lambda$ = 1.5), does the DTD follow a power-law shape of t^{-1}. If $\alpha_{CE} \geq 1.5$, we may obtain a power-law DTD, while for α_{CE} = 1.0 ($\alpha_{CE}\lambda$ = 0.5), not only does the shape not follows a power-law shape, but the birth rate is also significantly lower than that for α_{CE} = 3.0 (see also Ruiter et al. 2009). This is because that a low α_{CE} generally means a more heavy shrinkage of the orbital separation to eject CE. The system is then more likely to merge into a single star, not a DD system. However, the birthrate is almost unaffected by variations in the delay time in the γ-algorithm, i.e. the DTD does not follow a power law. In the γ-algorithm, the separation of a DD system surviving a CE phase is usually larger than that in the α-formalism (see Eq. (3)), which leads to a very long GWR timescale, and then a lower birth rate within 15 Gyr. It is noteworthy to point out that the γ-algorithm favors the production of SNe Ia with a long delay time (Meng et al. 2011b). When α_{CE} = 3.0, about two thirds of the SNe Ia explode within 1 Gyr, which is qualitatively consistent with observations (see the review of Maoz & Mannucci 2011), while in the other two cases, the SNe Ia older than 1 Gyr are more common.

In Fig. 1, there is a single spike at early times, because the SNe Ia with delay times shorter than 10^8 yr are very rare for the DD channel. To save CPU time, we defined a binary sample to be 10^7 binaries. If we enlarge the sample to be large enough, the single spike should disappear and the line become continuous.

We also check the dependence of the DTD shape on metallicity, finding little significant influence using both the α-formalism and γ-algorithm. Figure 2 shows the effect of metallicity on the DTD of α_{CE} = 3.0. We note that for the SNe Ia with the shortest delay time, a high metallicity leads to a systematically earlier explosion time of SNe Ia, which is mainly due to the effect of metallicity on the stellar structure. For these SNe Ia, their delay time is dominated by the evolutionary time of the primordial secondary and the contribution of GWR is negligible. For a certain evolutionary stage, a star with a high metallicity generally has a larger radius, and may then fill its Roche lobe earlier. Hence, a given binary system with a high metallicity usually enters the CE phase earlier. If a DD system survives the CE evolution, an earlier explosion is expected. Another feature in Fig. 2 is that low metallicity generally leads to a SN Ia with a long delay time, especially for those older than ∼1.5 Gyr, which results in a shallower power law at low metallicity. This also reflects the effects of metallicity on the stellar evolution. Generally, a star with a low metallicity usually produces a more massive white dwarf, i.e. a less massive CE (Meng, Chen & Han 2008). After CE ejection, the surviving DD system of low metallicity has a larger orbital separation than that of high metallicity. Although a more massive WD also has a shorter GWR timescale, the separation is the dominant factor when determining the GWR timescale, and a large orbital separation then means a longer GWR timescale.

In Fig. 2, we compare our power-law DTDs with recent observations. Our results are marginally consistent with observations.

3.2. Birth rate for a constant star formation rate

Figure 3 shows the Galactic birth rates of SNe Ia (i.e. Z = 0.02 and SFR = 5.0 $M_{\odot}$ yr^{-1}) from the DD channel. In the figure, the Galactic birth rate is around 0.5–3.0 × 10^{-3} yr^{-1}, which is marginally consistent with that inferred from observations (3–7 × 10^{-3} yr^{-1}, van den Bergh & Tammann 1991; Cappellaro & Turatto 1997; Li et al. 2011). For the case of α_{CE} = 3.0, the SNe Ia start at the age of several tens of Myr and the birth rate increases remarkably until about 0.2 Gyr. The birth rate then slowly increases, again because SNe Ia with short delay times predominate the case of α_{CE} = 3.0. However, for the other two cases, the birthrates permanently increase with delay time, owing to most of SNe Ia having a long delay time.

Figure 4 presents the effects of metallicity on the birth rate of SNe Ia with a constant SFR of 5 $M_{\odot}$ yr^{-1}. From the figure, we can see that decreasing the metallicity from 0.02 to 0.0001 may increase the present birth rates by up to about 50%, which is qualitatively consistent with the discovery that the SN Ia rate in lower-metallicity galaxies is higher than that in metal-rich environments (Kister et al. 2011). However, the present birth rate does not monotonically increase with decreasing metallicity, i.e. the highest value is for the case of Z = 0.002. The reason for this phenomenon is that explained in the above section, i.e. a low metallicity may lead to a longer GWR timescale. If the

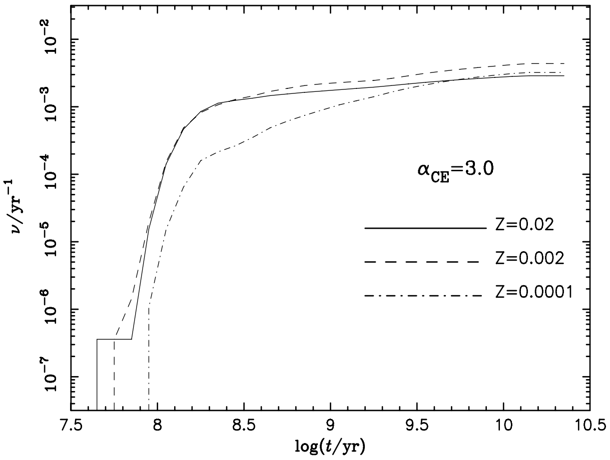

Fig. 4. The evolution of the birth rates of SNe Ia for a constant star formation rate (SFR = 5 $M_{\odot}$ yr^{-1}) with different metallicities, where α_{CE} = 3.0. Solid, dashed, and dot-dashed lines show the cases of Z = 0.02, 0.002, and 0.0001, respectively.

Table 1. DTD normalization(N_{SN}/M_{*}) from DD mergers for different metallicities and different treatments of CE in unit of $10^{-3}/M_{\odot}$.

Z	α_{CE} = 1.0	α_{CE} = 3.0	γ_{CE} = 1.5
0.02	0.098	0.58	0.26
0.002	0.13	0.87	0.24
0.0001	0.22	0.64	0.29

GWR timescale of DD system is so long that its delay time is longer than 15 Gyr, it does not contribute to the present birth rate of SNe Ia. Interestingly, the DD system was proposed to be the progenitor of super-luminous SNe Ia (Astier et al. 2006; Howell et al. 2006), which tend to explode in metal-poor environments (Khan et al. 2011b).

3.3. The normalization of DTD

Apart from the form of the DTD, there is also fairly good agreement in terms of the DTD normalization N_{SN}/M_{*}, i.e. the time-integrated number of SNe Ia per stellar mass formed. The range of its value is (0.5–3.5) × $10^{-3}/M_{\odot}$, focusing on 2 × $10^{-3}/M_{\odot}$ (Maoz & Mannucci 2011). In Table 1, we present the DTD normalization for DD mergers with different metallicities and different treatments of CE evolution. The results here are again marginally consistent with those from observations. The upper limit to the DTD normalization here is only 0.87 × $10^{-3}/M_{\odot}$, which is true for the case of Z = 0.002 and α_{CE} = 3.0.

3.4. The DTD from SD + DD

In Fig. 5, we show a DTD obtained from a combination of the SD and DD scenarios, where the SD scenario includes the WD + He star, WD + MS, and WD + RG channels and the mass transfers for these channels all occur via a stable RLOF between a WD and helium/main sequence/redgiant star, not by wind accretion (see Wang et al. 2009 and Meng & Yang 2010a in details). For the WD + He star channel in Wang et al. (2009), a helium star is in helium main sequence or crosses the helium HG. As in the DD channel, the DTD from the SD channel is also affected by the treatment of CE, so is the combined DTD. For α_{CE} = 1.0, the SD channel dominates the SNe Ia with a short delay time, while

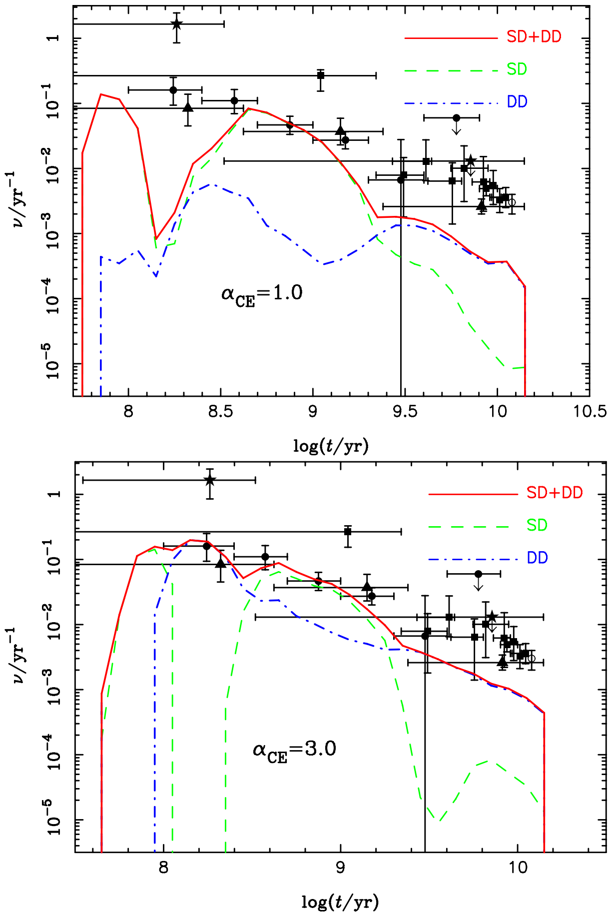

Fig. 5. The evolution of the birth rate of SNe Ia for a single starburst of $10^{11} M_{\odot}$ and Z = 0.02. Solid, dashed, and dot-dashed lines are from SD + DD, SD, and DD channels, respectively. The results for the SD channel are from Wang et al. (2009) and Meng & Yang (2010a) including the WD + He star, WD + MS, and WD + RG channels, while those for the DD channel are from this paper. The circle is from Mannucci et al. (2005), the filled circles are from Totani et al. (2008), stars are from Maoz & Badenes (2010), squares are from Maoz et al. (2010), and triangles are from Maoz et al. (2011). *Top*: α_{CE} = 1.0. *Bottom*: α_{CE} = 3.0.

the DD channel contributes most of the SNe Ia older than about 2 Gyr. The final combined DTD is a weak bimodality, where the WD + He star channel mainly contributes to SNe Ia with delay times shorter than 0.1 Gyr, WD + MS to those of 0.1–2 Gyr and DD channel to those older than 2 Gyr. At delay time shorter than 2 Gyr, this combined DTD is not inconsistent with observations for large observational errors, but the long delay-time part of the DTD is significantly lower than observations by a factor up to 10. For α_{CE} = 3.0, the combined DTD is closely consistent with the observational data for SNe Ia with delay times shorter than 2 Gyr, while for the SNe Ia older than 2 Gyr, the combined DTD only marginally matches observations. As in the case of α_{CE} = 1.0, the DD channel is also the dominant channel for the SNe Ia older than 2 Gyr. The contribution of the WD + RG channel could be neglected (see also Lipunov et al. 2011). However, for young and middle age SNe Ia, the contributions of the SD and DD scenarios are comparable.

3.5. The distribution of total mass

Howell (2011) suggested that the DD scenario has a natural explanation for a relatively high SN luminosity in young

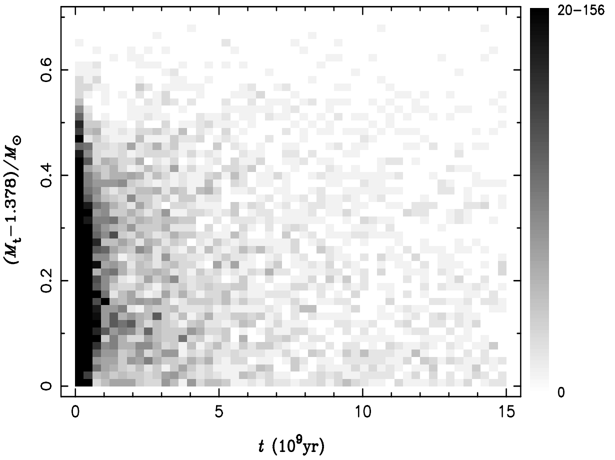

Fig. 6. The evolution of the distribution of the total mass of the DD systems leading to SNe Ia for a single starburst, where $Z = 0.02$ and $\alpha_{\rm CE} = 3.0$. In the figure, all the cells move downward artificially by 1.378 $M_{\odot}$.

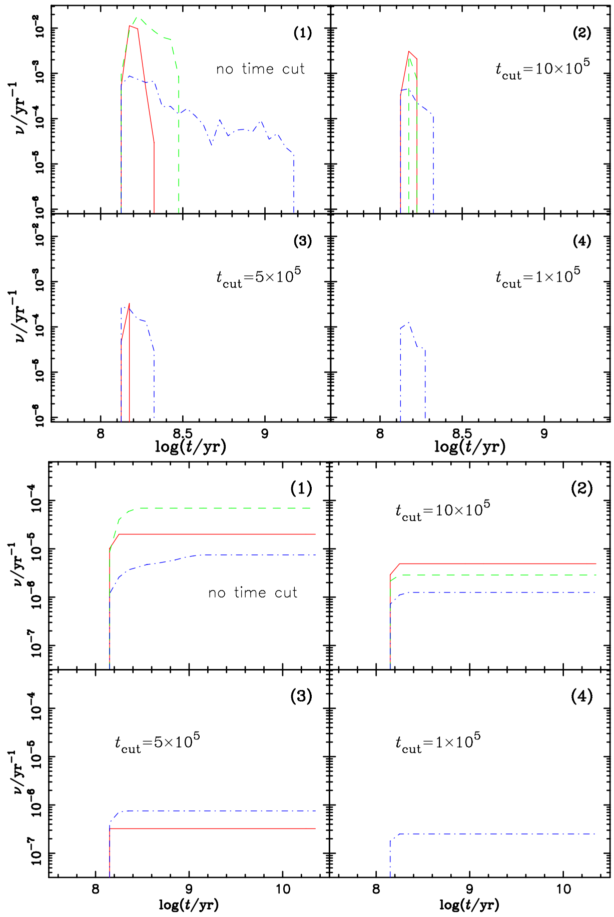

Fig. 7. The evolution of the birth rate of SNe Ia from a CD channel for a single starburst of 10^{11} $M_{\odot}$ (*top*) and constant star formation rate of 5 $M_{\odot}\,{\rm yr}^{-1}$ (*bottom*) with different cutting times and different treatments of the CE, where $Z = 0.02$. The delay time in the figure does not include the spinning-down time from magneto-dipole radiation. Solid, dashed, and dot-dashed lines are the cases of $\alpha_{\rm CE} = 2.0$, $\alpha_{\rm CE} = 3.0$, and $\gamma_{\rm CE} = 1.5$, respectively.

environments, namely that younger, more massive stars produce more massive white dwarfs, which have more potential fuel than less massive mergers, and then brighter SNe Ia (see also Maoz & Mannucci 2011). If this suggestion were right, we should see a significant change in the total mass range of DD systems and its average value, i.e. the range and intermediate value of the total mass should decrease with delay time. In Fig. 6, we show the evolution of the distribution of the total mass, but we do not find any significant expected evolution, i.e. the distribution of the total mass is rather uniform across the whole delay-time interval. The uniform distribution is produced mainly because the dominant delay time for SNe Ia from DD systems is determined by the GWR, not the evolutionary time of the secondary.

We investigated various physical properties when searching for a correlation between delay time and a mass-dependent quality (the masses of more massive WD M_1, less massive one M_2, mass ratio M_2/M_1, reduced mass $\frac{M_1 M_2}{M_1+M_2}$, the radius of less massive WD, the final separation when coalescence begins, and the total angular momentum of the system at the moment of the onset of coalescence). Despite our efforts, no correlation fulfills the observational limit (the range of the parameter decreases with the age of the SNe Ia, while the average value of the parameter decreases/increases with the age) was found, which has roots in the evolution of the total mass and mass ratio distributions. Hence, under the framework of DD scenario, it may still be difficult to explain the scatter in the brightness of the SNe Ia or the Phillips relation and more efforts are needed to build a bridge between the DD model and explosion model of SNe Ia.

In Fig. 6, most of the DD systems have a mass higher than the Chandrasekhar mass by no more than 0.5 $M_{\odot}$. During the merging process of a DD system, the less massive WD is generally destroyed and its mass is accreted onto the more massive WD. On the basis of Shen et al. (2012), we could expect that after the destruction of the less massive WD, a giant-like structure be produced during the accretion stage. Because of the relatively long-lasting time that the giant-like structure persists, we might expect to lose about half a solar mass from the system (Soker 2011). If this were a real scenario, according to the results in Fig. 6, the final masses of the most mergers could not reach the Chandrasekhar mass, and the SNe Ia could not then be expected, even though the total mass of the DD systems before merging exceeds the Chandrasekhar mass limit.

4. The birth rate of SNe Ia from CD systems

4.1. Without spinning-down time

In Fig. 7, we show the evolution of the birth rate of SNe Ia from the CD channel for a single starburst and a constant star formation rate with different treatments of CE, where the spinning-down time from magneto-dipole radiation is assumed to be insignificant and SN Ia occurs immediately after merging. The cutting time means that only when a CD system merges within the cutting time, is it assumed to explode as a SNe Ia. In the figure, almost all of the SN Ia produced by CD systems have a delay time shorter than 2×10^8 yr and the birth rate peaks at $\sim 1.5 \times 10^8$ yr if we assume that all the potential CD systems must merge within 10×10^5 yr after the CD systems form, where the delay time is mainly determined by the evolutionary time of the primordial secondary whose primordial mass is generally higher than 3 $M_{\odot}$. Hence, if a spinning-down time following magneto-dipole radiation did not play a dominant role on the delay time of SNe Ia, the CD scenario may only produce SNe Ia with very short delay times as expected by Livio & Riess (2003). In panel (1) of Fig. 7, some SNe Ia may have delay times as long as 1.5 Gyr, especially for $\gamma_{\rm CE} = 1.5$, which is from the "pollution" channel. Our results for cutting times shorter than 10×10^5 yr are not polluted by the channel.

Even in the case of $t_{\rm cut} \leq 10 \times 10^5$ yr, the results are still significantly affected by the treatment of CE evolution. For a α-formalism, if $\alpha_{\rm CE} < 2.0$, no CD system survives the CE evolution. Even for $\alpha_{\rm CE} \geq 2.0$ ($\alpha_{\rm CE}\lambda \geq 1.0$), the CD systems that survived CE evolution will always merge within a timescale longer than 1×10^5 yr. In contrast, the γ-algorithm may produce CD systems with various merger timescales.

However, the peak value of the birth rate for the CD channel is lower than that for the normal DD channel by 1–3 magnitudes, which means that the SNe Ia produced in the CD scenario are not the main contributors to all SNe Ia. As shown in the bottom figure of Fig. 7, no more than 1 in 1000 SNe Ia should be produced by the CD scenario. The low birth rate results from the constraint that the more massive hot core originates from the primordial secondary.

4.2. With spinning-down time

Ilkov & Soker (2012) suggested that the delay time for SNe Ia produced by a CD system may be dominated by the spin-down timescale related to magneto-dipole radiation torque, and the timescale from an initial fast rotation Ω_0 to a critical angular velocity $\Omega_{\rm c}$ is

$$\tau_{\rm B} \approx 10^8 \left(\frac{B}{10^8\ {\rm G}}\right)^{-2} \left(\frac{\Omega_{\rm c}}{0.7\Omega_{\rm Kep}}\right)^{-2} \times \left(\frac{R}{4000\ {\rm km}}\right)^{-1} \left(\frac{\sin\delta}{0.1}\right)^{-2} \left(\frac{\beta_{\rm I}}{0.3}\right) \left[1 - \left(\frac{\Omega_0}{\Omega_{\rm c}}\right)^{-2}\right] {\rm yr}, \quad (5)$$

where B is the magnetic field, R is the radius of WD, and $\beta_{\rm I}$ is a structural constant for the moment of inertia. For simplicity, we assume that $\Omega_0 = \Omega_{\rm Kep}$, $\Omega_{\rm c} = 0.7\Omega_{\rm Kep}$, $\beta_{\rm I} = 0.3$, and R = 4000 km. The spin-down timescale is then

$$\tau_{\rm B} \approx 5 \times 10^7 \left(\frac{B \sin\delta}{10^7\ {\rm G}}\right)^{-2} {\rm yr}, \quad (6)$$

where $B \sin\delta$ follows a distribution of

$$\frac{{\rm d}N}{{\rm dlog}(B\sin\delta)} = {\rm const.}, \quad (7)$$

for 10^6 G $\leq B\sin\delta \leq 10^8$ G (Ilkov & Soker 2012). On the basis of this distribution, we obtained the spin-down timescale using a Monte Carlo simulations, and inferred the delay time of a SN Ia to be the sum of the evolutionary timescale in forming a CD system, the one for GWR, and the spin-down timescale if the total mass of the CD system is lower than 1.48 $M_\odot$ otherwise the spin-down timescale is neglected for those with total masses higher than 1.48 $M_\odot$ (Yoon & Langer 2004).

In Fig. 8, we show the DTD of SNe Ia produced by a CD system, where the spin-down timescale is included. In the figure, the DTD also follows a power law of t^{-s}, where s ranges from 1.0 to 1.5 depending on the treatment of CE evolution. This is a natural result since the distribution of the $B\sin\delta$ is deduced from a power-law DTD (Ilkov & Soker 2012). Hence, the spin-down timescale is very important to the SNe Ia produced by the CD channel since the power-law shape does not occur according to the α-formalism if the spin-down timescale is not taken into account (see Fig. 7). In addition, as expected by Kashi & Soker (2011) and Ilkov & Soker (2012), a few SNe Ia produced by CD systems may have delay times as long as several Gyr.

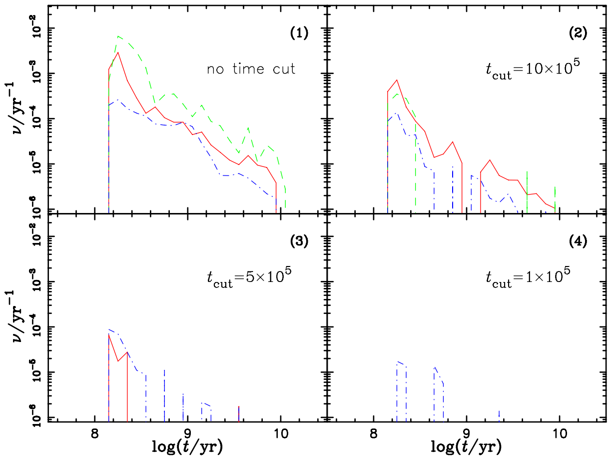

Fig. 8. The evolution of the birth rate of SNe Ia from the CD channel for a single starburst of $10^{11} M_\odot$ with different cutting times and different treatments of CE, where $Z = 0.02$. The delay time in the figure includes the spinning-down time from magneto-dipole radiation. Solid, dashed, and dot-dashed lines are the cases for $\alpha_{\rm CE} = 2.0$, $\alpha_{\rm CE} = 3.0$, and $\gamma_{\rm CE} = 1.5$, respectively.

5. Discussions and conclusions

5.1. Other possible channels for SNe Ia

From our study, we have found that the birth rate of SNe Ia for DD channels may only be marginally consistent with observations, and the rate depends significantly on the treatments of CE. Only when $\alpha_{\rm CE} \geq 1.5$, may we obtain a DTD whose shape follows a power law of t^{-1}, and the birth rate is only consistent with the lower limit of this trend derived from observations. For the cases of $\alpha_{\rm CE} < 1.5$ and $\gamma_{\rm CE} = 1.5$, neither the DTD shapes nor the birth rates match the available observations. Badenes & Maoz (2012) calculated the merger rate of binary WDs in the Galactic disk based on observational data in the Sloan Digital Sky Survey and concluded that the merger rate of binary WDs with super-Chandrasekhar masses would not control significantly the SNe Ia rate. Our results are qualitatively consistent with the calculations of Badenes & Maoz (2012). If we consider the contribution of the SD channel as done in Mennekens et al. (2010), the combination DTD may match observations for delay times $t < 2.5$ Gyr, at least within observational errors, regardless of the value of $\alpha_{\rm CE}$. However, when $t > 2.5$ Gyr, the birth rate from combination DTD is lower than that from observations. Therefore, other channels or mechanisms may contribute to SNe Ia with long delay times.

In this paper, the WD + He star, the WD + MS, and the WD + RG channels are included for the SD channel, while the wind-accretion channel is exclued. Chen, Han & Tout (2011) constructed a tidally-enhanced wind-accretion model where the initial mass of RG donor may be as low as 1 $M_\odot$, i.e. the delay time from the channel may be as long as 10 Gyr. On the basis of Eq. (1) of Iben & Tutukov (1984), they obtained a birth rate of 6.9×10^{-3} yr^{-1} from the wind model. Although we believe that the birth rate is probably overestimated since some parameter spaces considered to be valid for SNe Ia production in Eq. (1) of Iben & Tutukov (1984) may not contribute to SNe Ia, the wind channel should improve our results in this paper.

Some overluminous SNe Ia were observed and a super-Chandrasekhar mass explosion was expected for these SNe Ia based on the amount of ^{56}Ni inferred (Astier et al. 2006; Howell et al. 2006; Hicken et al. 2007; Scalzo et al. 2010; Yuan et al. 2010; Tanaka et al. 2010; Yamanaka et al. 2010). These overluminous SNe Ia are most likely to occur in metal-poor environments (Khan et al. 2011b). Although they are generally assumed to be produced by the coalescence of DD systems, they may also originate in SD systems (Chen & Li 2009; Liu et al. 2009; Hachisu et al. 2012). However, the super-Chandrasekhar mass explosion from the SD channel may only contribute to SNe Ia with short delay times (Hachisu et al. 2012), and their contribution to all SNe Ia may be no more than 0.3% (Meng et al. 2011b).

5.2. The effect of metallicity

As noted in Sects. 3.1 and 3.2, the birth rate of SNe Ia depends on metallicity, especially for those with long delay times. Meng et al. (2011a) found that decreasing the metallicity may significantly increase the birth rate of SNe Ia with long delay times, that are produced by the WD + RG channel, by a factor of about three. Some observations do indeed find that a lower metallicity may correspond to a higher SNe Ia birth rate (Kistler et al. 2011).

The picture emerging from some observations is remarkable, i.e. most of these diverse DTD derived from different methods, different environments, and different redshifts agree with each other, in both form and absolute value (Maoz & Mannucci 2011; Graur et al. 2011). At delays of $t > 1$ Gyr, a power law of index about -1 seems to be in little doubt, although a index of ~ -1.5 could not be ruled out (Barbary et al. 2012; Sand et al. 2012), while at delays $t < 1$ Gyr, the shape of the DTD might become either shallower or steeper, or follow the same shape seen at long delays. In this paper, we note that for the DD scenario, a low metallicity may lead to a shallower DTD. Interestingly, for a SD channel, a shallower DTD may also be obtained at low metallicity (Meng et al. 2011a). In addition, metallicity may also affect the value of the birth rate of SNe Ia (Kistler et al. 2011). Nevertheless, the level of the effect of metallicity on the DTD might not be as high as we expect (see in Fig. 2) since the DTDs from different environments agree with each other. However, we still have to determine using observations the precise effect of metallicity on the DTD since metallicity does have an influence on the DTD, on both its form and absolute value, and then the shape of the DTD at delays $t < 1$ Gyr might become clear.

5.3. The origin of the Phillips relation

The Phillips relation is the most fundamental relation when a SN Ia is used as a distance indicator, which implies that the properties of SNe Ia are mainly dominated by one parameter. However, the nature of this parameter remains unclear (Podsiadlowski 2008). Many efforts have been made to resolve this problem, but most of these discussions have focused on the Chandrasekhar mass model, in which the WDs explode as SNe Ia when their masses are close to the Chandrasekhar mass limit. No consensus has yet been reached at present. Here, we tried to identify a parameter in the DD scenario to explain the scatter in the luminosity of SNe Ia. Unluckily, no such a parameter was found. In particular, the total mass of the DD systems is a poor choice of parameter to illustrate the dependence of the average luminosity of SNe Ia on their age. Hence, the origin of Phillips relation still remains unclear.

5.4. The birth rate of SNe Ia from CD channel

We have found that the upper limit to the contribution of the SNe Ia produced by the CD channel to the total SNe Ia is only about 0.1%. One may argue that this result may seriously depend on the treatment of CE evolution since the treatment here is very simple and the real scenario may be very complex (Kashi & Soker 2011; Passy et al. 2012). At present, it remains very difficult to construct a more complete model in a BPS study. However, since the simple treatment may succeed in reproducing the forms of many special objects, such as planetary nebulae and subdwarf B stars (Han et al. 1995, 2002, 2007), the results here could be reasonable to at least first order.

However, one may remark that since the CD systems had hardly survived the CE evolution, we might ignore the systems that almost survive the CE evolution, especially for a lower $\alpha_{\rm CE}$. These systems might also explode if their spinning-down time is long enough to permit the remaining CE material to be lost by a wind. Because the results of 0.1% is derived from the α-formalism of $\alpha_{\rm CE} \geq 2.0$, we might underestimate the birth rate of SNe Ia predicted by the CD scenario. However, if $\alpha_{\rm CE} < 2.0$, no CD system can survive the CE evolution. This is a natural result since a low $\alpha_{\rm CE}$ means that a system needs to shrink its separation more dramatically and release more orbital energy to eject the CE. We do not verify whether this merger occurs because this would require consideration of the details of CE evolution and many assumptions have to be made, which may lead to too many uncertainties. Fortunately, our results place a constraint on the problem. For a high $\alpha_{\rm CE}$, the systems that merge under the situation of low $\alpha_{\rm CE}$ could survive, while those surviving the CE evolution with low $\alpha_{\rm CE}$ may lead to a larger orbital separation. Hence, the panel (1) in Figs. 7 and 8 should give a safe upper limit on the birth rate of SNe Ia based on the CD scenario, where all the potential CD systems should be included. Even so, the total contribution from all the potential CD systems to all SNe Ia is no more than 1%. In addition, the spin-down mechanism is very important to the DTD shape of SNe Ia derived for the CD systems, especially for the α-formalism. We cannot obtain a power-law form if the spin-down timescale due to the magneto-dipole radiation torque is not taken into account.

In summary, we have calculated the evolution of the birth rate of SNe Ia from DD and CD channels. We found that the treatment of the CE evolution has a great influence on the final DTD shape, and only for the α-formalism when $\alpha_{\rm CE} \geq 1.5$, the shape of the DTD is consistent with that derived from observations, but the birth rate of this case only marginally matches that derived observationally. For a α-formalism with a lower $\alpha_{\rm CE}$ and the γ-algorithm, the birth rate of SNe Ia from DD systems is much lower than those derived from observations, and the shape of the predicted DTD does not follow a power law. Metallicity has almost no influence on the shape of DTD except in terms of the index of the power law, but may increase the value of the birth rate of SNe Ia. When the SD channel including WD + He star, WD + MS, and WD + RG channels is incorporated, the theoretical DTD matches the observations very well for SNe Ia younger than 2.5 Gyr, while for those older than 2.5 Gyr, the theoretical birth rate is slightly lower than that derived from observations. We also need to incorporate other channels or mechanisms that contribute to the SNe Ia explosion. As suggested by Soker (2011) and Ilkov & Soker (2012), the CD scenario is a possible channel contributing to SNe Ia and we have found three potential channels that may produce the CD systems. However, the strict upper limit to the contribution from the CD scenario to all SNe Ia is 1%.

Acknowledgements. We are very grateful to the anonymous referee for his/her constructive suggestions, which improved the manuscript greatly. This work was partly supported by the Natural Science Foundation of China (11003003), the Project of Science and Technology from the Ministry of Education (211102), and the Key Laboratory for the Structure and Evolution of Celestial Objects, Chinese Academy of Sciences.

References

Arnett, W. D. 1982, ApJ, 253, 785
Astier, P., Guy, J., Regnault, N., et al. 2006, A&A, 447, 31
Badenes, C., & Maoz, D. 2012, ApJ, 749, L11
Barbary, K., Aldering, G., Amanullah, R., et al. 2012, ApJ, 745, 32
Brandt, T. D., Tojeiro, R., Aubourg, E., et al. 2010, AJ, 140, 804
Branch, D., & Bergh, S. V. 1993, AJ, 105, 2231
Bravo, E., Domínguez, I., Badenes, C., et al. 2010a, ApJ, 711, L66
Cappellaro, E., & Turatto, M. 1997, in Thermonuclear Supernovae, eds. P. Ruiz-Lapuente, R. Cannal, & J. Isern (Dordrecht: Kluwer), 77
Cappellaro, E., Turatto, M., Tsvetkov, D. Y., et al. 1997, A&A, 322, 431
Chen, X., & Han, Z. 2002, MNRAS, 335, 948
Chen, X., & Han, Z. 2003, MNRAS, 341, 662
Chen, X., & Han, Z. 2008, MNRAS, 387, 1416
Chen, W., & Li, X. 2009, ApJ, 702, 686
Chen, X., Han, Z., & Tout, C. A. 2011, ApJ, L31
de Kool, M., van den Heuvel, E. P. J., & Pylyser, E. 1987, A&A, 183, 47
Gallagher, J. S., Garnavich, P. M., Caldwell, N., et al. 2008, ApJ, 685, 752
Graur, O., Poznanski, D., Maoz, D., et al. 2011, MNRAS, 417, 916
Hachisu, I., Kato, M., Hideyuki, S., & Nomoto, K. 2012, ApJ, 744, 69
Hamuy, M., Phillips, M. M., Schommer, R. A., et al. 1996, AJ, 112, 2391
Han, Z. 1998, MNRAS, 296, 1019
Han, Z., Podsiadlowski, P., & Eggleton, P. P. 1995, MNRAS, 272, 800
Han, Z., Tout, C. A., & Eggleton, P. P. 2000, MNRAS, 319, 215
Han, Z., Podsiadlowski, Ph., Maxted, P. F. L., Marsh, T. R., & Ivanova, N. 2002, MNRAS, 336, 449
Han, Z., Podsiadlowski, Ph., & Lynas-Gray, A. E. 2007, MNRAS, 380, 1098
Hicken, M., Garnavich, P. M., Prieto, J. L., et al. 2007, ApJ, 669, L17
Hillebrandt, W., & Niemeyer, J. C. 2000, ARA&A, 38, 191
Höflich, P., Gerardy, C. L., Marion, H., & Quimby, R. 2006, New Astron. Rev., 50, 470
Höflich, P., Krisciunas, K., Khokhlov, A. M., et al. 2010, ApJ, 710, 444
Howell, D. A. 2011, NatCo, 2E, 350
Howell, D. A., Sullivan, M., Nugent, P. E., et al. 2006, Nature, 443, 308
Howell, D. A., Conley, A., Della Valle, M., et al. 2009a [arXiv:0903.1086]
Howell, D. A., Sullivan, M., Brown, E. F., et al. 2009b, ApJ, 691, 661
Hoyle, F., & Fowler, W. A. 1960, ApJ, 132, 565
Hurley, J. R., Pols, O. R., & Tout, C. A. 2000, MNRAS, 315, 543
Hurley, J. R., Tout, C. A., & Pols, O. R. 2002, MNRAS, 329, 897
Hjellming, M. S., & Webbink, R. F. 1987, ApJ, 318, 794
Iben, I., Jr., & Tutukov A. V. 1984, ApJS, 54, 335
Ilkov, M., & Soker, N. 2012, MNRAS, 419, 1695
Ivanova, N. 2011, ASPC, 447, 91
Kasen, D., Röpke, F. K., & Woosley, S. E. 2010, Nature, 460, 869
Kashi, A., & Soker N. 2011, MNRAS, 417, 1466
Khan, R., Stanek, K. Z., Prieto, J. L., et al. 2011a, ApJ, 726, 106
Khan, R., Stanek, K. Z., Stoll, R., et al. 2011b, ApJ, 737, L24
Kistler, M. D., Stanek, K. Z., Kochanek, C. S., et al. 2011 [arXiv:1106.3115]
Krueger, B. K., Jackson, A. P., Townsley, D. M., et al. 2010, ApJ, 719, L5
Kuznetsova, N., Barbary K., Connolly, B., et al. 2008, ApJ, 673, 981
Landau, L. D., & Lifshitz, E. M. 1962, The Classical Theory of Fields (Oxford: Pergamon)
Leibundgut, B. 2000, A&ARv, 10, 179
Lesaffre, P., Han, Z., Tout, C. A., et al. 2006, MNRAS, 368, 187
Li, W. D., Chornock, R., Leaman, J., et al. 2011, MNRAS, 412, 1473
Lipunov, V. M., Panchenko, I. E., & Pruzhinskaya, M. V. 2011, New Astron., 16, 250
Liu, W., Chen, W., Wang, B., & Han, Z. 2010, A&A, 523, A3
Livio, M., & Riess A. 2003, ApJ, 594, L93
Livio, M., & Soker, N. 1988, ApJ, 329, 764
Mannucci, F., Della Valle, M., Panagia, N., et al. 2005, A&A, 433, 807
Maoz, D., & Badenes, C. 2010, MNRAS, 407, 1314
Maoz, D., & Mannucci, F. 2011 [arXiv:1111.4492]
Maoz, D., Sharon, K., & Gal-Yam, A. 2010, ApJ, 722, 1879
Maoz, D., Mannucci, F., Li, W., et al. 2011, MNRAS, 412, 1508
Mazzali, P. A., Nomoto, K., Cappellaro, E., et al. 2001, ApJ, 547, 988
Mazzali, P. A., Röpke, F. K., Benetti, S., & Hillebrandt, W. 2007, Science, 315, 825
Meng, X., & Yang, W. 2010, ApJ, 710, 1310
Meng, X., & Yang, W. 2011, A&A, 531, A94
Meng, X., Chen, X., & Han, Z. 2008, A&A, 487, 625
Meng, X., Li, Z., & Yang, W. 2011a, PASJ, 63, L31
Meng, X., Chen, W., Yang, W., & Li, Z. 2011b, A&A, 525, A129
Miller, G. E., & Scalo, J. M. 1979, ApJS, 41, 513
Mennekens, N., Vanbeveren, D., De Greve, J. P., & De Donder, E. 2010, A&A, 515, A89
Neill, J. D., Sullivan, M., Howell, D. A., et al. 2009, ApJ, 707, 1449
Nelemans, G., & Tout, C. A. 2005, MNRAS, 356, 753
Nelemans, G., Verbunt, F., Yungelson, L. R., et al. 2000, A&A, 360, 1011
Nomoto, K., Thielemann, F.-K., & Yokoi, K. 1984, ApJ, 286, 644
Nomoto, K., Umeda, H., Hachisu, I., et al. 1999, in Type Ia Suppernova: Theory and Cosmology, eds. J. Truran, & T. Niemeyer (New York: Cambridge Univ. Press), 63
Nomoto, K., Uenishi, T., Kobayashi, C., et al. 2003, in From Twilight to Highlight: The Physics of supernova, ESO/Springer serious, ESO Astrophysics Symposia, eds. W. Hillebrandt, & B. Leibundgut (Berlin: Springer), 115
Paczyński, B. 1976, in Structure and Evolution of Close Binaries, eds. P. P. Eggleton, S. Mitton, & J. Whelan (Dordrecht: Kluwer), 75
Parthasarathy, M., Branch, D., Jeffery, D. J., & Baron, E. 2007, New Astron. Rev., 51, 524
Passy, J., De Marco, O., Fryer, C. L., et al. 2012, ApJ, 744, 52
Perlmutter, S., Aldering, G., Goldhaber, G., et al. 1999, ApJ, 517, 565
Phillips, M. M. 1993, ApJ, 413, L105
Pinto, P. A., & Eastman, R. G. 2001, New Astron., 6, 307
Podsiadlowski, P., Rappaport, S., & Pfahl, E. D. 2002, ApJ, 565, 1107
Podsiadlowski, P., Mazzal,i P. A., Lesaffre, P., et al. 2006 [arXiv:astro-ph/0608324]
Podsiadlowski, P., Mazzali, P., Lesaffre, P., Han, Z., & Förster F. 2008, New Astron. Rev., 52, 381
Riess, A. G., Filippenko, A. V., Challis, P., et al. 1998, AJ, 116, 1009
Riess, A., Kirshner, R. P., Schmidt, B. P., et al. 1999, AJ, 117, 707
Riess, A., Strolger, L.-G., Casertano, S., et al. 2007, ApJ, 659, 98
Ruiter, A. J., Belczynski, K., & Fryer, C. 2009, ApJ, 699, 2026
Ruiter, A. J., Belczynski, K., Sim, S. A., et al. 2011, MNRAS, 417, 408
Sand, D. J., Graham, M. L., Bildfell, C., et al. 2012, ApJ, 746, 163
Scalzo, R. A., Aldering, G., Antilogus, P., et al. 2010, ApJ, 713, 1073
Schmidt, B. P., Suntzeff, N. B., Phillips, M. M., et al. 1998, ApJ, 507, 46
Shanks, T., Allen, P. D., Hoyle, F., et al. 2002, ASPC, 283, 274
Shen, K. J., Bildsten, L., Kasen, D., et al. 2012, ApJ, 748, 35
Sim, S. A., Röpke, F. K., Hillebrandt, W., et al. 2010, ApJ, 714, L52
Soker, N. 2011 [arXiv:1109.4652]
Sparks, W. M., & Stecher, T. P. 1974, ApJ, 188, 149
Tanaka, M., Kawabata, K. S., Yamanaka, M., et al. 2010, ApJ, 714, 1209
Timmes, F. X., Brown, E. F., & Truran, J. W. 2003, ApJ, 590, L83
Totani, T., Morokuma, T., Oda, T., et al. 2008, PASJ, 60, 1327
Tout, C. A., Aarseth, S. J., Pols, O. R., & Eggleton, P. P. 1997, MNRAS, 291, 732
Travaglio, C., Hillebrandt, W., & Reinecke, M. 2005, A&A, 443, 1007
van den Bergh, S., & Tammann, G. A. 1991, ARA&A, 29, 363
Wang, B., & Han, Z. 2012, New Astron. Rev., 56, 122
Wang, L., Höflich, P., & Wheeler, J. C. 1997, ApJ, 483, L29
Wang, B., Chen, X., Meng, X., & Han, Z. 2009, ApJ, 701, 1540
Webbink, R. F. 1984, ApJ, 277, 355
Webbink, R. 1985, in Interacting Binary Stars, eds. J. E. Pringle, & R. A. Wade (Cambridge University Press), 39
Webbink, R. F. 1988, in The Symbiotic Phenomenon, eds. J. Mikolajewska, M. Friedjung, S. J. Kenyon, & R. Viotti (Dordrecht: Kluwer), 311
Webbink, R. 2008, in Short-Period Binary Stars: Observations, Analyses, and Results, eds. E. F. Milone, et al. (Berlin, Germany: Springer), 233
Whelan, J., & Iben, I. 1973, ApJ, 186, 1007
Yamanaka, M., Kawabata, K. S., Kinugasa, K., et al. 2010, ApJ, 707, L118
Yoon, S., & Langer, N. 2004, A&A, 419, 623
Yuan, F., Quimby, R. M., Wheeler, J. C., et al. 2010, ApJ, 715, 1338
Yungelson, L., & Livio, M. 2000, ApJ, 528, 108
Zorotovic, M., Schreiber, M., & Gänsiche, B. 2010, A&A, 520, A86